

Design, Fabrication and Implementation of a
Flexure-based Micropositioner for Dip Pen Nanolithography

by

Marcel A.C. Thomas

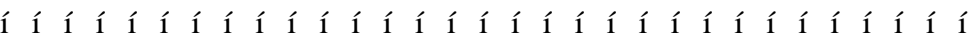
Submitted to the Department of Mechanical Engineering
in Partial Fulfillment of the Requirements for the Degree of
Bachelor of Science in Mechanical Engineering

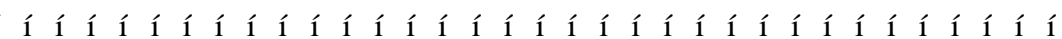
at the

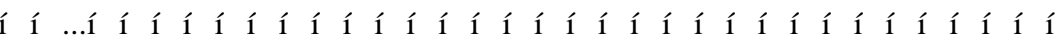
Massachusetts Institute of Technology

June 2012

© 2012 Massachusetts Institute of Technology
All rights reserved.

Signature of Author 
Department of Mechanical Engineering
May 25, 2012

Certified by 
Martin L. Culpepper
Associate Professor of Mechanical Engineering
Thesis Supervisor

Accepted by  ...
Professor John H. Lienhard V
Samuel C. Collins Professor of Mechanical Engineering
Undergraduate Officer

Design, Fabrication and Implementation of A
Flexure-based Micropositioner for Dip Pen Nanolithography

by

Marcel A.C. Thomas

Submitted to the Department of Mechanical Engineering
on May 25, 2012 in Partial Fulfillment of the
Requirements for the Degree of Bachelor of Science in
Mechanical Engineering

ABSTRACT

Dip Pen Nanolithography (DPN) takes the concept of a quill-tip pen and shrinks it to the nanometer scale. DPN uses a machine to pick up and deposit proteins and liquids in arrays. A problem with the machine however is aligning the pen tip relative to the machine. Currently, it is aligned manually, which is time and labor intensive. It would drastically increase productivity and throughput if a machine was developed that could perform this task accurately and repeatedly. This would also allow quick tool changes for experiments involving multiple DPN processes. The impact of this alignment machine is that it solves problems not only for DPN machines, but also for atomic force microscopes and similar instruments. This thesis is about the design and implementation of this alignment machine. The user would arbitrarily place the pen tip on a ball mount. The ball mount would have three holes that are larger than three balls. The balls are held stationary, while the ball mount can move over it. An overhead camera is used to determine the actual and desired position of the ball mount relative to the balls. Once the ball mount reaches its desired position, the balls are glued in place using UV-cured epoxy. This half of a kinematic coupling would then attach to the other half of a kinematic coupling on the DPN machine. The repeatability of the ball mount holder was tested and has an in-plane 1 translational repeatability of 15.9 μm and 0.0122 rad. This can be improved and further work is suggested.

Thesis Supervisor: Martin L. Culpepper
Title: Professor of Mechanical Engineering

ACKNOWLEDGEMENTS

I would like to acknowledge the advice and leadership of Professor Martin Culpepper. The opportunity to work on this project was an invaluable learning experience for me. I have also learned a great deal from a UROP that I did in the spring of my junior year, which inspired me to continue working with professor Culpepper, both for this thesis and for graduate studies. Professor Culpepper's advice has furthered my development in engineering and academia, and for that I will be forever grateful.

I would also like to acknowledge the work of John Hopkins in FACT (Freedom and Constraint Topologies). His work in this area directly led me to a large beneficial design change in this project.

Lastly, I would like to thank the staff of some machine shops on campus: the Pappalardo Lab and the MIT Hobby Shop. The Pappalardo shop staff (Jim Dudley, Bill Cormier, Steve Haberek, Joe Cronin, and of course Dick Fenner) offered friendly, knowledgeable advice that led to the completion of the prototype. The staff of the MIT Hobby Shop (Ken Stone, Hayami Arakwa, and Brian Chan) also provided a wealth of advice and support throughout this project.

CONTENTS

Abstract	3
Acknowledgements.....	5
Contents.....	7
Figures	9
Tables.....	10
1.....	11
1.1 Dip Pen Nanolithography Background.....	11
1.2 Kinematic Coupling Background	13
1.3 Overall Design Idea	13
2.....	15
2.1 Functional Requirements	15
2.1.1 Degrees of Freedom	15
2.1.2 Amount of travel	16
2.2 Ball Mount Holder.....	17
2.2.1 In-plane holder	18
2.2.2 Out-of-plane holder	19
2.3 Flexure Design	19
2.3.1 Flexure Topology.....	20
2.3.2 Wire Flexure Analytical Model	21
2.3.3 FEA	21
2.3.4 Natural Frequency Analysis	22
2.3.5 Stiffness	23
2.3.6 Buckling	23
2.3.7 Stress	24
2.4 Actuation.....	24

2.5	Ground Assembly	26
2.5.1	Ground Plate	26
2.5.2	Ball Mount Pedestal Holder	26
2.6	UV Light Mount	27
2.7	Camera Assembly	27
2.8	Controls	28
2.9	Full Assembly.....	29
3	30
3.1	Fabrication.....	30
3.2	Assembly.....	31
4	32
4.1	Experimental Design.....	32
4.2	Results	33
4.3	Conclusion from Testing.....	35
5	37
5.1	Summary	37
5.2	Future Work	38
References	40

FIGURES

Figure 1.1: The DPN Process [1].	12
Figure 1.2: Fundamental Design Idea.	14
Figure 2.1: Coordinate System [3].	15
Figure 2.2: Sources of Error by Placing the Tip on the Ball Mount.	16
Figure 2.3: The Ball Mount Holder.	18
Figure 2.4: In-Plane Holder.	18
Figure 2.5: Bottom of Out of plane Ball Mount Holder.	19
Figure 2.6: Appropriate FACT Topology [2].	20
Figure 2.7: FEA Model of the Flexure.	22
Figure 2.8: Natural Frequency Modes of the Flexure.	22
Figure 2.9: A Buckling Simulation.	24
Figure 2.10: Model of the Voice Coils Implemented with the Flexural Stage.	25
Figure 2.11: Ground Assembly Model.	26
Figure 2.12: The UV Mount Assembly Model.	27
Figure 2.13: The Camera Assembly Model.	28
Figure 2.14: The Control Loop for the Positioning System.	29
Figure 2.15: A CAD Rendering of the Full Assembly.	29
Figure 3.1: Pockets for a Kinematic Coupling were post-machined using a CNC mill after the part was Waterjetted.	30
Figure 3.2: The Fabricated Assembly.	31
Figure 4.1: The Base Image of the Pen Tip for Repeatability Testing.	33
Figure 4.2: In-Plane Repeatability Results.	34
Figure 4.3: Translational Repeatability Results.	35

TABLES

Table 2.1: Translational Requirements.	17
Table 2.2: Translational Stiffness.	23
Table 2.3: Rotational Stiffness.....	23
Table 4.1: 1 and 3 Repeatability Measurements.....	35

INTRODUCTION

The purpose of this research was to develop a machine that makes miniature kinematic couplings for alignment for micromanufacturing processes. The research covered here encompassed the modeling, optimization and fabrication of this machine. The import of this machine is that it allows for accurate, repeatable interchange of parts for various nanoscale instruments, such as Dip Pen Nanolithography (DPN) and Atomic Force Microscopy. This will improve the quality, rate, and flexibility of these instruments while decreasing the cost of alignment methods. This research was divided into two phases, design and implementation. The design, covered in chapter 2, contains the ideas and optimization of all of the parts that comprise the alignment machine. The implementation contains the fabrication, assembly, and testing of the parts of this machine.

1.1 Dip Pen Nanolithography Background

Dip Pen Nanolithography takes the concept of a quill pen and shrinks it to the nanometer scale. An atomic force microscope cantilevered tip acts as the pen, a chemical compound of interest acts as the ink and a substrate acts as the paper. The pen tip is so small that it can pick up and deposit proteins and small liquid droplets in regular arrays. The arrays can be of complex, user-defined shapes with features as small as 50 nm or as large as 10 μ m. The substrates that can be used for DPN include glass, plastic and silicon. DPN is flexible enough to print organic, inorganic, and biological materials. These materials include proteins, nucleic acids, lipids, hydrogels, polymers, and nanoparticles. DPN could either print molecules directly, or it can print materials through a liquid carrier. For molecular inks, varying the meniscus size and the tip-surface contact time controls the feature size, resulting in features of a size between 50 nm and as

large as 1 μm . For liquid carriers, the feature size is controlled by varying the liquid-surface affinity, the surface contact time and environmental conditions [1].

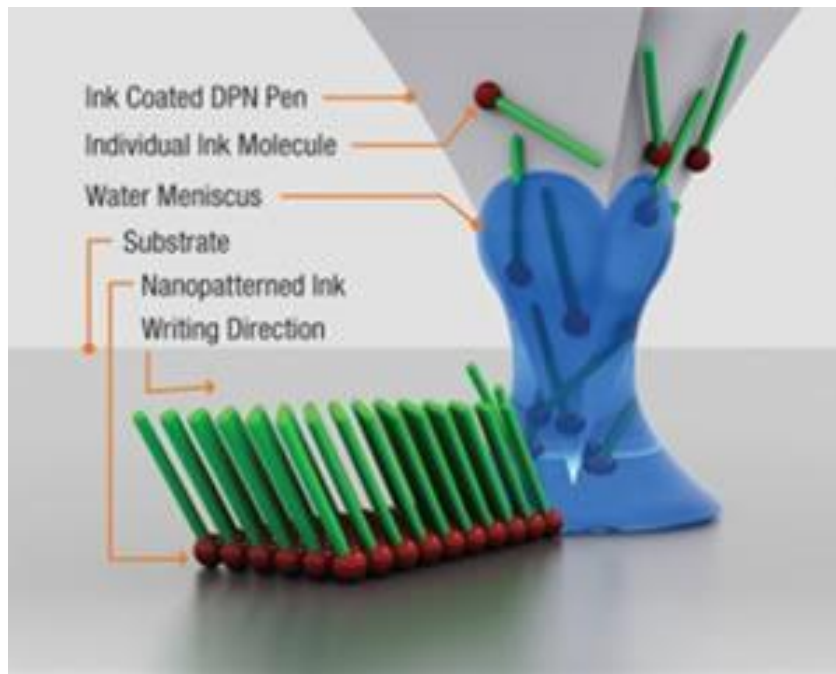


Figure 1.1: The DPN Process [1].

Advantages that DPN has over other nanomanufacturing techniques include: it is simple to use, the DPN machine is benchtop-sized, it achieves patterning techniques without the need for a cleanroom, a master stamp, or a photomask, and it can operate under ambient conditions. The applications of DPN include sensor and microstructure functionalization, nanofabrication, protein analysis, cell biology, and biomaterials. Furthermore, DPN can be used in conjunction with other micro- and nanomanufacturing techniques. Although DPN is additive (the structures are built from the bottom-up), and usually prints on an ordinary flat surface, DPN can also be used to print directly onto existing micro- and nanostructures including sensors, PDMS stamps, microfluidic arrays, or photomasks. This allows for complex microstructures to be developed that are comprised of top-down and bottom-up features. Examples of structures where this is suitable include nanoscale diffraction gratings, plasmonic features, and arbitrary solid-state patterns.

Despite the numerous advantages that DPN presents, the machine used by NanoInk (a company that specializes in nanometer scale manufacturing through DPN) has a mechanical problem. The problem is aligning the pen tip relative to the machine. The pen tips need to be

aligned to 1 μm accuracy and 0.1 μm repeatability. Currently, it is aligned manually, which is time and labor intensive. It would drastically increase productivity and throughput if a machine was developed that could perform this task accurately and repeatably. This research is about the design and implementation of this machine. The user would arbitrarily place the pen tip on a ball mount. The ball mount would have three holes that are larger than three balls. The balls are held stationary, while the ball mount can move over it. An overhead camera is used to determine the actual and desired position of the ball mount relative to the balls. Once the ball mount reaches its desired position, the balls are glued in place using UV-cured epoxy. This half of a kinematic coupling would then attach to the other half of a kinematic coupling on the DPN machine.

1.2 Kinematic Coupling Background

The NanoInk DPN machine needs a fixture for the pen tip that has high accuracy and repeatability. A well-known, high performance fixture is a kinematic coupling. Kinematic couplings have proven themselves to be reliable, simple, inexpensive means of connecting parts with high repeatability. A kinematic coupling uses exact constraint to align two parts with respect to each other. Every rigid body has six degrees of freedom: three for translation and three for rotation. Exact constraint shows that as long as there are six non-redundant points of contact between two objects and a nesting force that pushes them into this points of contact, then the objects can repeatably and accurately be located with respect to each other. The way a kinematic coupling achieves the six $\tilde{\text{points}}$ of contact is through balls and grooves. The spheres provide a point of tangency against a plane. There are several methods of exact constraint coupling: passive kinematic couplings, active kinematic couplings, quasi-kinematic couplings, compliant kinematic couplings, elastic averaging, and pinned joints. Due to its simplicity in fabrication, moderate stiffness, and high repeatability, a passive kinematic coupling was used chosen for the alignment machine. The disadvantages of the kinematic coupling include high stress concentration at the contact points and do not allow for sealed joints, however, kinematic couplings can be designed to suit this application.

1.3 Overall Design Idea

The kinematic coupling ensures repeatability, but accuracy is the main concern. The heart of the machine came from the idea to align the pen tip relative to a part, and then put the part into

the machine in a repeatable way. The part used is one half of a kinematic coupling, the other half is on the machine. This method of introducing an intermediate stage allowed for the possibility of quickly changing tools to perform multiple experiments. The addition of an intermediate stage posed a problem with alignment, namely that the pen tip has to be aligned relative to the machine, so even if the tip is aligned well to the intermediate stage, if the intermediate stage is not aligned well relative to the NanoInk machine, then the alignment machine is useless. How well the parts had to be aligned with respect to each other is detailed in the functional requirements in Chapter 2.

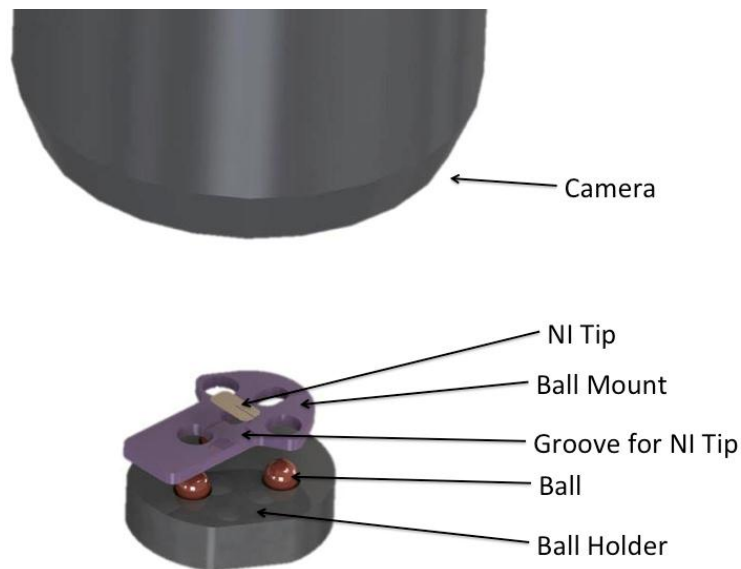


Figure 1.2: Fundamental Design Idea.

2.1 Functional Requirements

The required degrees of freedom for the machine were identified, as well as the required amount of movement in those directions. Also, repeatability and accuracy required were assessed.

2.1.1 Degrees of Freedom

The pen tip was applied onto the kinematic coupling in a planar fashion. Therefore, the dominant error is going to come from the planar directions, namely X, Y, and z , shown in Figure 2-2.

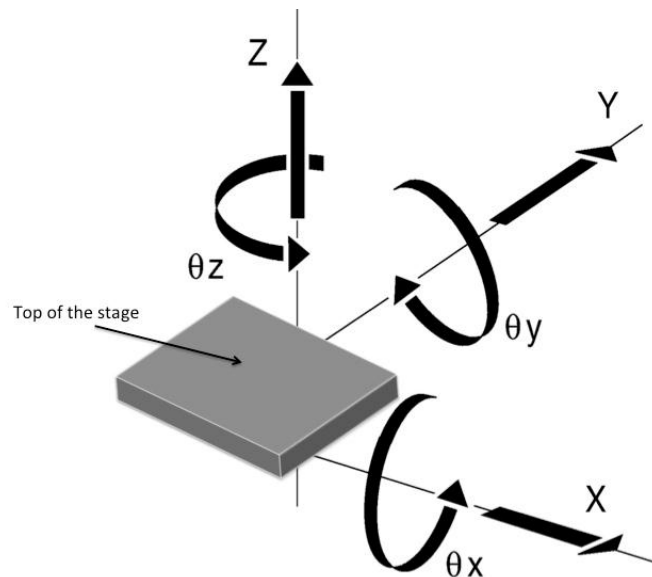


Figure 2.1: Coordinate System [3].

Since the region of interest is a point (the pen tip), at first it did not seem necessary to control z , i.e., it seemed much more important to control X and Y. However, z prove to be important for certain pens that had multiple tips. The other degrees of freedom (Z , x , and y) will not be a part of the first design, but if they are deemed necessary, they can be added in later. For this design iteration, only the in-plane motion was considered.

2.1.2 Amount of travel

To figure out how much travel the stage needs, the tolerances of the mating parts were considered, namely, the NanoInk Tip tolerances, and the tip holder machining tolerances. This gave the ball holder tolerance and the stage travel requirements.

To get the NanoInk Tip tolerances, several tips were measured with a micrometer. The length and the width were measured for six samples. The sample size was small because the method of measurement could ruin the tips by crushing them and each tip is quite expensive. Although the measurement technique was crude, it erred on the side of caution. That is, it caused a large deviation, which led to a conservative estimate of how far the stage had to travel. It was found that the length was a constant 3.607 mm. The width was an average of 1.605 mm. The maximum width was 0.132 mm larger than the average, and the smallest was 0.096 mm smaller than the average. Thus, the width tolerance is roughly 0.006 inches. The machining tolerances come from the machines used to fabricate the ball mount holder. The machine used for fabrication was a CNC Mill, which has a tolerance of roughly 0.001 inches.

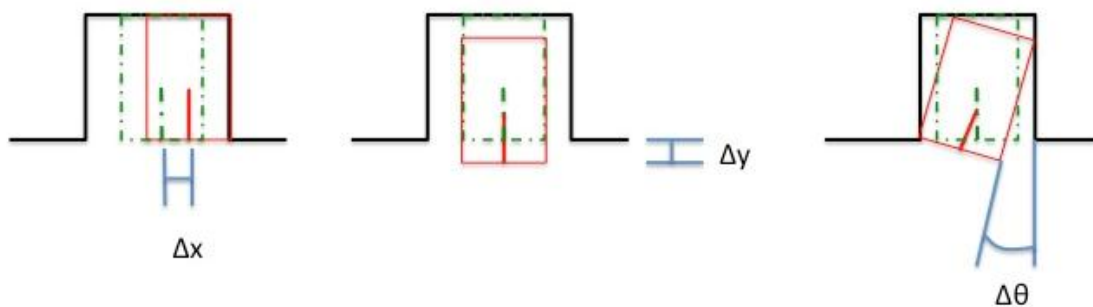


Figure 2.2: Sources of Error by Placing the Tip on the Ball Mount.

The X translation is given by

$$\begin{aligned}
 X &= ((\text{nominal tip size} \ominus \text{smallest tip size}) + \text{compensation} + \text{machining tolerances}) / 2 \quad (2.1) \\
 &= ((1.605\text{mm} \ominus 1.511\text{mm}) + 0.152\text{mm} + 0.025\text{mm}) / 2 \\
 &= 0.136\text{mm} \\
 &= 136 \text{ microns}
 \end{aligned}$$

The error in Y comes from length tolerances, machining tolerances, and placement error, which is uncontrolled. Thus, the oversized tolerance undetermined, but the undersized tolerance comes from machining, so it is approximately 25 microns. Since the upper limit is unbounded, for simplicity, the upper limit is the same as it is for X, namely 136 microns.

The travel in z involves some trigonometry, but it can be shown that the required angle is approximately 0.1 radians (6°). Also, the translation that results from this angular offset is significant, namely it was roughly 6 times the error estimated in translation alone. Thus, in controls, the angular offset gets corrected first, and then the translational error is corrected. To account for any other sources of error (e.g. assembly errors, manufacturing errors, etc.), a safety factor of 2 is implemented. The worst-case scenario is that the ball mount is outside the view of the camera, but the functional requirements are well within that scope. The stage travel requirements are summarized in Table 2.1.

Table 2.1: Translational Requirements.

	Travel
X	272 m
Y	272 m
z	0.2 rad

2.2 Ball Mount Holder

The ball mount needed to be held stationary relative to the main stage. This was achieved through the ball mount holder. The holder used flexures to push the ball mount against hard stops in six directions to control all six degrees of freedom. This mount was comprised of two parts: an in-plane holder and an out-of-plane holder.



Figure 2.3: The Ball Mount Holder.

2.2.1 In-plane holder

The in-plane holder quasi-kinematically controlled the in plane degrees of freedom by having flexural beams pushing against three bumps. The bumps are positioned such that they do not interfere with the pen tip. The in-plane holder has three slots on its perimeter that pointed towards the center. These slots aligned the holder relative to the stage using dowel pins to diminish errors in assembly. The in-plane holder is held out of the plane of the stage with three bolts. The in-plane holder is shown in Figure 2.5.

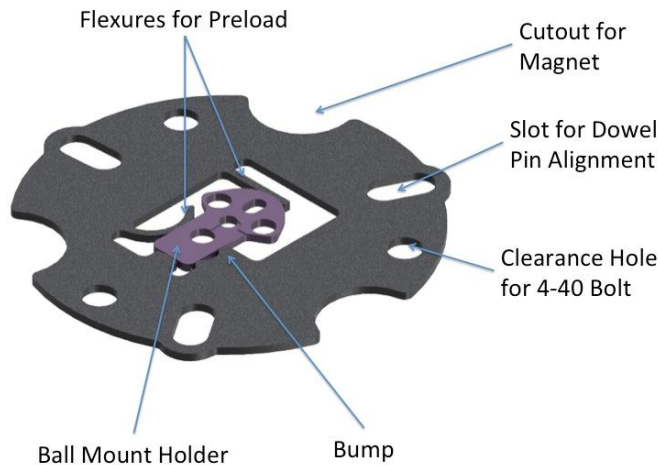


Figure 2.4: In-Plane Holder.

2.2.2 Out-of-plane holder

The out-of-plane holder uses three flexures to push the ball mount from the top onto a thin plate. This prevented the ball mount from moving out of plane. The preload was maintained through magnets. This feature allows the machine operator to quickly remove the ball mount and load a new ball mount into the holder. There were three magnets to constrain the out-of-plane holder out of the plane of the stage. There are three slots for alignment in the plane of the stage through the use of dowel pins. The magnets are placed such that one of them has the polarity flipped from the other two. This way, the operator cannot place the out of plane holder such that the flexures do not interfere with the balls or the pen tip. A rendering of the bottom of the out-of-plane holder is shown in Figure 2.6.

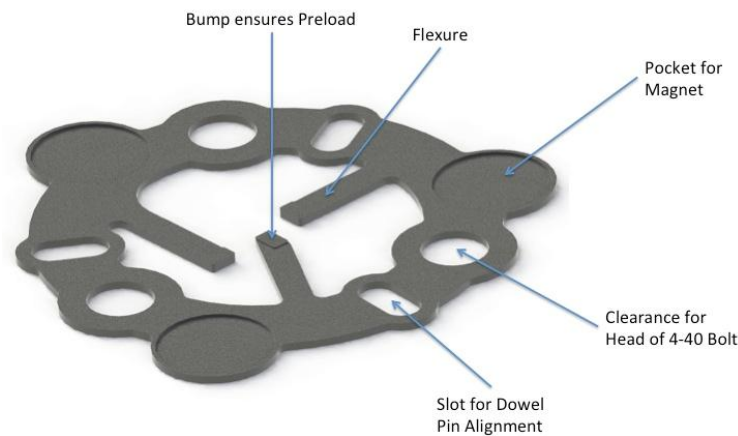


Figure 2.5: Bottom of Out of plane Ball Mount Holder.

2.3 Flexure Design

For such small displacements, it was desirable to implement flexures. Flexures are basically beams that act as springs. Springs are desirable because displacement is linearly related to a force via the spring stiffness. Thus, an actuator with a known force output (e.g. a voice coil) can be selected. Using the force from the actuator and the required displacement, the required stiffness can be derived. For beams, the stiffness is a function of material (Young's Modulus) and geometry (thickness, width, and length). The material chosen was aluminum since it is inexpensive and easy to machine. By altering geometry, the beams can be designed to be much

stiffer in one direction than another. Then, by arranging these beams in clever ways, relative constraint can be ascertained in some directions, while achieving relative compliance in other directions. Jon Hopkins developed a method, called Freedom and Constraint Topologies (FACT), for arriving at the arrangement of these flexures for the desired degrees of freedom. [2]

2.3.1 Flexure Topology

The topology of the flexure was derived from principles of FACT, and a well-known clever trick for linear motion. The appropriate degrees of freedom were established, and, according to FACT, using wire flexures minimized the stiffness in plane, while maximizing stiffness out of plane. The flexures were made by waterjetting thin sheet metal. Because the sheet metal is so thin, the flexures can be produced quickly, easily, and cheaply. This is advantageous because if the flexure is excessively stiff or the actuators are underpowered, then a thinner flexure can be produced.

Finding the appropriate degrees of freedom for the stage, and then finding the appropriate “Freedom Space” that matched it was the first step in using FACT. Luckily, the Freedom Space was obtained in a parallel flexure system, which allowed a simple, elegant design to emerge. This Freedom Space is only obtained through a complementary Constraint Space, which gives insight as to how the flexures should be arranged [2].

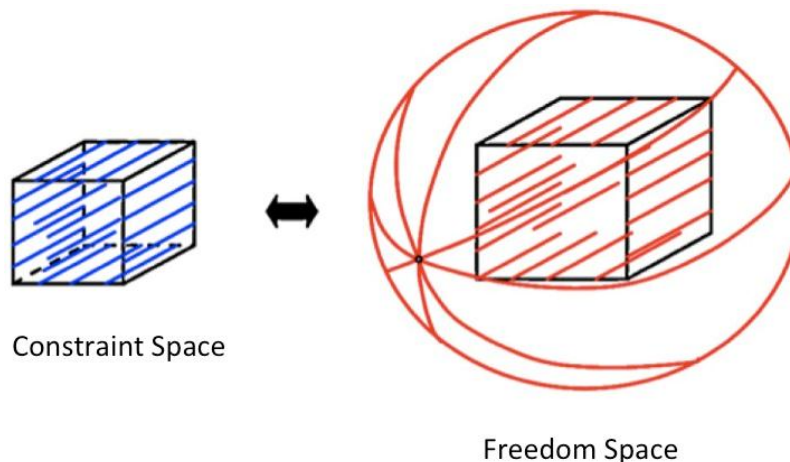


Figure 2.6: Appropriate FACT Topology [2].

A special trick was also used for linear motion. Normally, the flexure for linear motion is the classic “four-bar” flexure, but this has the problem of moving on an arc rather than in a line. That is, as it moves in the desired direction, it also dips. But by putting these two four-bar

flexures in series, then the arc error cancels out, leading to the desired linear motion. This trick was implemented in this flexure design. By using wire flexures, this trick works in both directions in the plane, X and Y.

2.3.2 Wire Flexure Analytical Model

For simple flexure designs, important flexure characteristics (e.g. stiffness) can be derived. Finite element analysis (FEA) can also give these values, but an analytical model is useful in that it illustrates the accuracy of the FEA. If the flexure does not exhibit the desired behavior, then the model is useful to show which parameters are more important than others, and by how much do they need to be changed to get the flexure to work. The stiffness in the X and Y directions were considered here. From beam bending, the stiffness of a beam under a fixed-guided end condition is given by

$$K = 2Eb \left(\frac{h}{L} \right)^3, \quad (2.2)$$

where E is the Young's modulus of the material, b is the width of the beam, h is the thickness, and L is the length of the beam. Since there are two sets of parallel beams in series, the stiffness in one direction is just given by the stiffness of one of the beams. The stiffness was chosen such that, given the force output of the chosen actuator, the stage could move to the desired displacement.

2.3.3 FEA

Solidworks Simulation was used to simulate the flexure before fabrication. To properly assess information about stiffness (particularly rotational stiffness), an assembly of the flexures and the stage was used (as opposed to just the flexure alone). Mesh Control was applied such that the wire flexure had at least four elements across the beam to properly capture information about stress and strain. When performing FEA, there is a trade-off between accuracy of the results and the time it takes to arrive at those results. That is, the finer the mesh is, the more accurate the results are, but the longer it takes. There is a point where the accuracy of the results converges to a value, while taking a minimal amount of time. Appropriate, approximate boundary conditions were used, namely that the bottom stage was held fixed and the parts of the assembly were globally bonded.

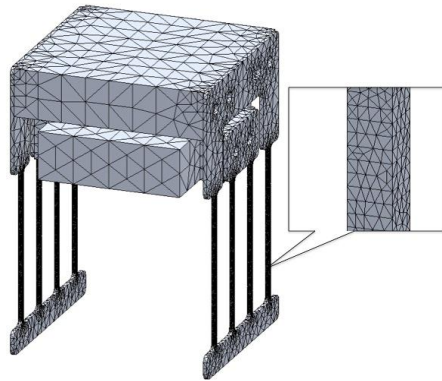


Figure 2.7: FEA Model of the Flexure.

2.3.4 Natural Frequency Analysis

The natural frequency was used to give a dynamic understanding of how the system will behave. The modes of vibration illustrated in what ways the flexure was least stiff. This was useful to show that the degrees of freedom were achieved.

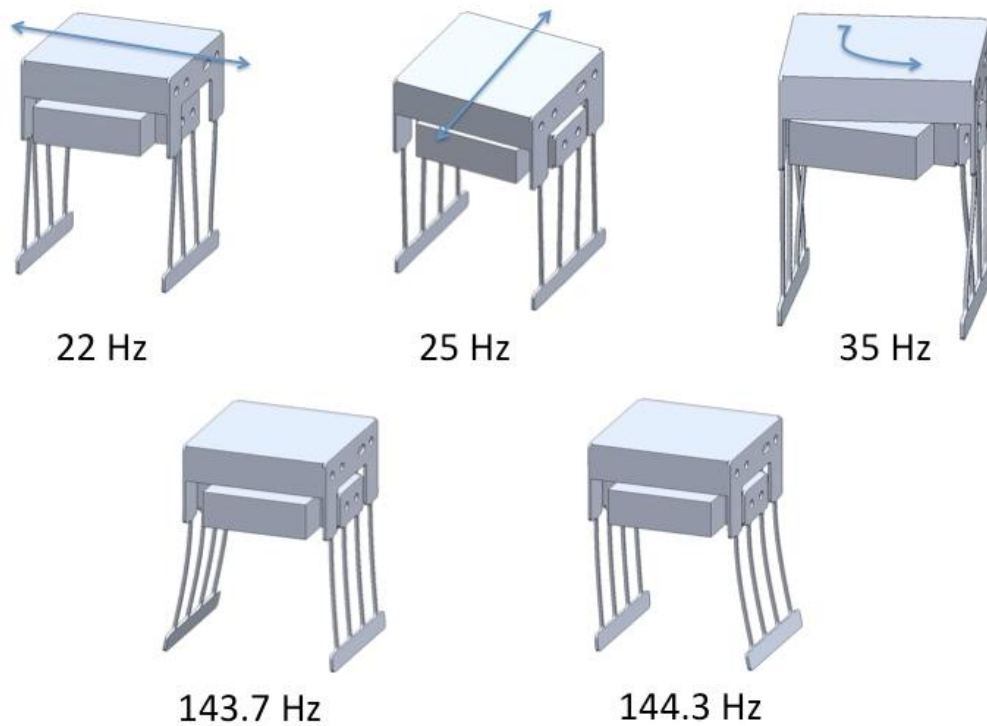


Figure 2.8: Natural Frequency Modes of the Flexure.

As shown, the directions in which it is least stiff are the degrees of freedom that are desired. The flexure is stiffer in Y than X because in the X direction, there is an extra cantilevered beam and there are no fillets. In the Y direction, the extra cantilevered beam is much stiffer. Furthermore, there are fillets in that direction that makes the flexure beams effectively shorter. The last two modes of vibration should really be the two bottom parts vibrating together, and the two bottom parts vibrating opposite to each other. The reason that they appear as depicted is because of asymmetry in the mesh. The mesh is not identical on both sides of the mesh, which led to asymmetry in the results. Despite the imperfections of the mesh, this flexure clearly displays the desired behavior and gave a quantitative idea of the resonant frequencies.

2.3.4 Stiffness

The stiffness of the flexures was found in FEA by applying a known force and measuring the displacement in the appropriate direction. For the torsional stiffnesses, the angle was not directly measured, so the angle was found from resultant displacement and trigonometry. The overall stiffnesses of the flexures in all directions are summarized in Table 2.1 and Table 2.2.

Table 2.2: Translational Stiffness.

	K (N/ m)
X	1.7×10^{-3}
Y	2.3×10^{-3}
Z	1.7

Table 2.3: Rotational Stiffness.

	K (Nm/rad)
x	220
y	1103
z	2

As desired, the stiffnesses in the required degrees of freedom were orders of magnitude smaller than the required directions of constraint.

2.3.5 Buckling

A buckling analysis was performed because the wire flexures are so long and thin (the aspect ratio is greater than 10.) The stiffness values for out-of-plane motion are only valid so

long as the beams did not buckle. The only force applied in the direction of buckling is the weight of the stage. The buckling load factor was approximately 80, meaning that there needs to be a force 80 times the weight of the stage to initiate buckling. Thus, the flexure will not buckle under normal operation, and the stiffness values are valid for normal use.

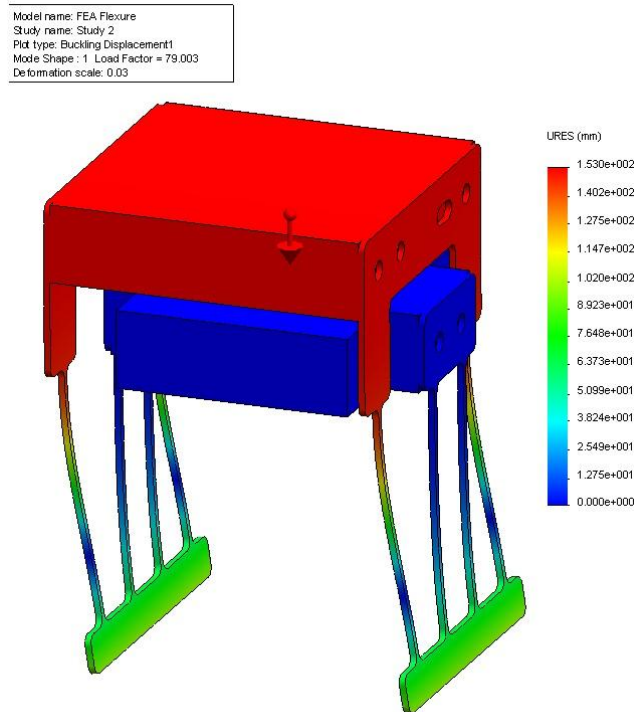


Figure 2.9: A Buckling Simulation.

2.3.6 Stress

To ensure that the flexure works well, it needs to deform to the required amount elastically. To ensure elasticity, the Von Mises stress needs to be lower than the yield stress. Thus, the flexure is designed such that it can move in twice its required range in its degrees of freedom while having a maximum stress that is less than the yield stress.

2.4 Actuation

Voice coils were chosen as the most appropriate actuator after reviewing several different types of actuators, namely, electrostatic, electromagnetic, piezoelectric, and thermomechanical.

For ease of implementation, the actuator needed to be meso-scale. Electrostatic actuators use electric fields to generate forces. They have low power consumption, but they are not suitable for multi-axis applications because of low force density and tight space constraints, namely the small gaps between the electrodes. The most common type of electrostatic actuator is the comb drive, which typically only provides tens of microns of travel with milli-Newtons of force [3,4,5]. This application requires over 100 microns of travel, which makes this type not feasible. Piezoelectric actuators required similar performance constraints, but with the additional hassle of fabrication complexity and poor reproducibility of material make-up [6]. Thermomechanical actuators can provided the range of travel and forces required, but they need a large, constant power consumption and a temperature range of more than 1000 K [7]. This temperature range causes significant thermal expansion in the flexures that affects the accuracy and reliability of this precision system. Electromagnetic actuation was the optimal choice because it provides high force and large stroke without the disadvantages listed above [8,9]. Voice coils are simple, meso-scale devices that are easy to implement. This is why they were chosen.

One voice coil was placed the X direction (the direction of least stiffness) and two voice coils were placed in the Y direction. By having both of the Y voice coils push by the same amount, then translation in Y is achieved. By having them push by different amounts (one pushing and one pulling), then the angle α_z is achieved. The voice coil arrangement is shown in Figure 2.11.

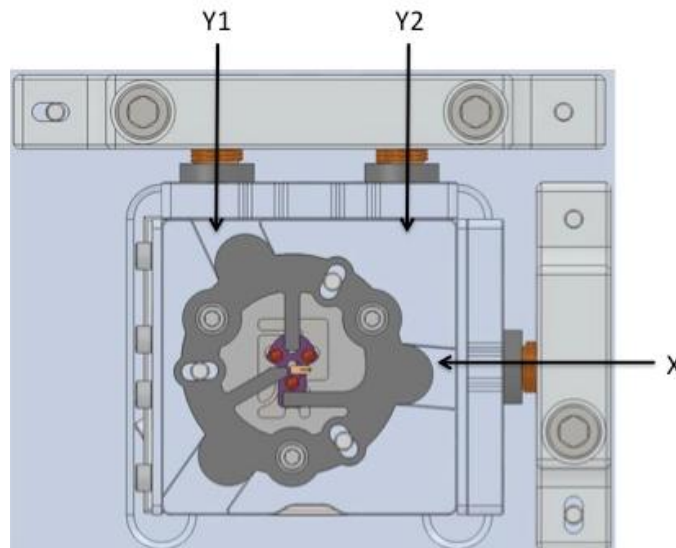


Figure 2.10: Model of the Voice Coils Implemented with the Flexural Stage.

2.5 Ground Assembly

The ground assembly consists of two main parts, the ground plate and the ball holder pedestal.

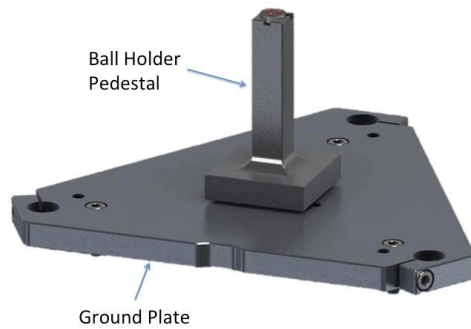


Figure 2.11: Ground Assembly Model.

2.5.1 Ground Plate

The ground plate can be bolted down to an optical table. However, the surface of the optical table is not flat, and neither is the ground plate. Thus, the surface-to-surface contact would cause the ground plate to warp, which causes the entire structure to warp. To eliminate that problem, instead of mating surfaces together, the surface of the optical table would be mated to three points on the ground plate. To approximate this condition, three islands were added underneath the ground plate.

2.5.2 Ball Mount Pedestal Holder

The ball mount pedestal was designed to go underneath the flexure and provide a rigid platform on which the balls were held. The ball holder mates with the top of the pedestal. They are two separate pieces because if the ball holder was damaged beyond repair, then that small part can be replaced, rather than replacing the relatively large, expensive, ball holder pedestal. There is a kinematic coupling that couples the pedestal to the ground. The kinematic coupling uses a magnet to achieve a known, constant preload. Rather than the traditional V-groove for the base, a pocket for dowel pins to be glued in was made. This method is easier to machine and it

provides a hardened, polished, steel surface for the balls to rest on, rather than machined aluminum.

2.6 UV Light Mount

The alignment machine moves the ball mount relative to the balls, and then UV epoxy is applied to fix the balls in place. Small UV flashlights were used to supply the UV light used in the epoxy curing process.

The UV light Mount was designed such that the light cones all intersected at the center stage. The ideal arrangement would be to use one flashlight at the center, but the camera lens has to be in the center, so a UV light was placed at an angle aiming towards the stage. This, however, created a shadow, thus three flashlights were placed such that the shadow of one light would be flooded with light by the other two flashlights. The parts were made out of the same thickness to make it easier and cheaper to manufacture.



Figure 2.12: The UV Mount Assembly Model.

2.7 Camera Assembly

The camera assembly went above the rest of the assembly and was vital for feedback. The repeatability and adjustability were essential. The camera chosen is quite sensitive for focusing, so a fine adjustment mechanism was needed.

The camera used was a CMOS Rolling Shutter camera. The camera has an active area of 570 by 428 microns and a resolution of 2592 by 1944 pixels. The camera has a pixel pitch of 2.2 by 2.2 microns. The frame rate is 7 Hz [10]. The problem with the frame rate is that the camera is too slow to capture the resonant frequencies of the flexure. Thus, the camera cannot be used for live feedback. However, it can be used for feedback by taking pictures of the stage. The control loop is described in section 2.9. The camera mount incorporates a kinematic coupling that allowed repeatable placement of the camera. The camera mount also has fine adjustment screws that allow the camera mount stage to tip and tilt. The adjustability is critical for this camera as the accuracy of the commands is derived by the quality of the image.

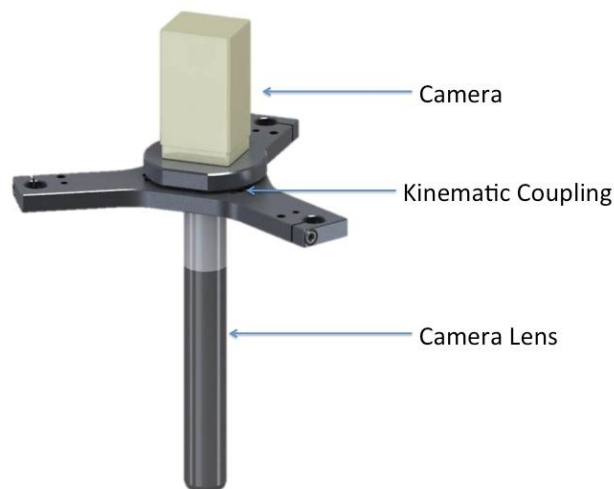


Figure 2.13: The Camera Assembly Model.

2.8 Controls

The location of the pen tip is derived from a picture taken by the camera. This image would then be sent to a LabView script that processed the image and compared where the pen tip is to where it should be. This script then calculates a x , y , and z , shown in Figure 2.3.

These values then get sent to a microcontroller (e.g. an Arduino) that would convert the required displacements into commands for current in the voice coils. These commands would then get sent to motor drivers that move the voice coils. Then, after the voice coil moves to its commanded position, the camera takes a picture of it again to close the feedback loop. If necessary, the entire loop is repeated until the required tolerance is reached. Because of the way

this loop works, it was deemed necessary to move the pen tip relative to the balls, as opposed to the other way around. Moving the balls relative to the pen tip requires knowledge of the pen tip and the position of the balls, which could be difficult to see if they are covered by glue.

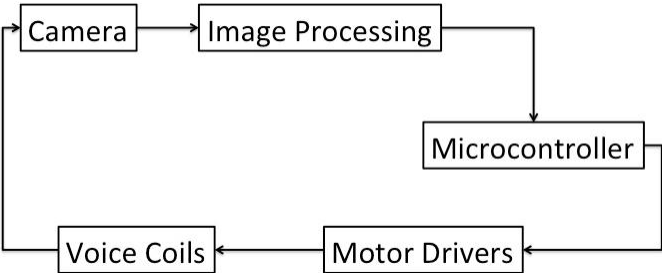


Figure 2.14: The Control Loop for the Positioning System.

2.9 Full Assembly

The full assembly takes all of the subassemblies and stacks them in a structure similar to a wedding cake. All of the structures are held in place with stainless steel rods. There are plastic tubes that act as spacers to define the heights of the various layers. A rendering of the CAD model is shown in Figure 2.16.



Figure 2.15: A CAD Rendering of the Full Assembly.

FABRICATION AND ASSEMBLY

3.1 Fabrication

Since the parts in the design were comprised of complex shapes and had tight tolerances, Computer Numerical Controlled (CNC) machines were used to fabricate the parts in the assembly. The CNC Machines used were a CNC Mill and the Waterjet. The CNC Mill was used to make the smaller parts, such as parts for the flexural stage. The Waterjet was used to make the flexures and the larger parts, such as the camera mount. The larger parts were so large, that they were awkward to fully fabricate in the Mill, so the Waterjet did most of the 2D machining, and then the Mill was used to make a couple of features. For example, pockets for the kinematic coupling and counterbores were made with a CNC Mill and holes for the structural rods were reamed.

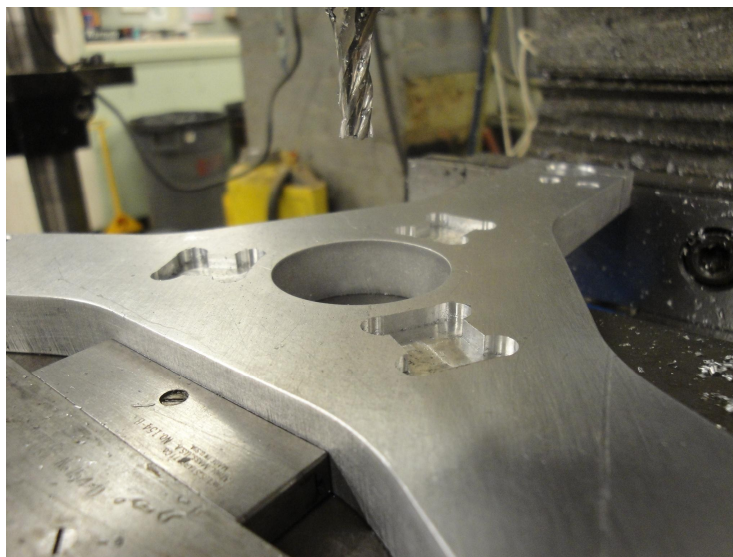


Figure 3.1: Pockets for a Kinematic Coupling were post-machined using a CNC mill after the part was Waterjetted.

3.2 Assembly

The machine was assembled in different modules and then those modules were assembled from the bottom up. That is, the ground plate was bolted to the table, and the ball pedestal was put on top. The ground poles are to be put in the three degree of freedom stage. The spacers were put on top of the ground plate and the stage assembly fits inside the holes in the spacers and ground. Then, the spacers for the UV light mount then slide onto the ground poles. Then the UV light mount slides onto the ground poles. Then the spacers for the camera adjustment were added, then the camera mount went on top. The camera was screwed into one half of the kinematic coupling for the camera mount. The lens then screwed into the camera by putting it through the hole in the UV light mount. Then, all of the sub-assemblies were barrel-clamped in place.

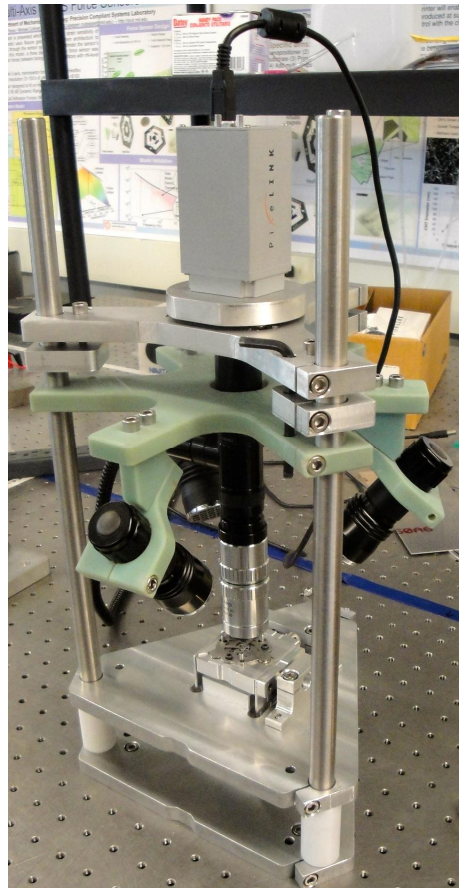


Figure 3.2: The Fabricated Assembly.

FIXTURE REPEATABILITY

4.1 Experimental Design

A high risk to the functionality of the machine is the repeatability of the ball mount holder. If the ball mount holder is not repeatable, then the flexure has to move farther than it was intended. The way to test these important aspects of this machine is to use the camera to test repeatability. The ball mount was put into and taken out of the ball mount holder repeatedly and the camera was used to measure the variation in its position relative to a reference feature. Image processing software measured the difference in position. The image processing software used was the National Instruments Vision Builder AI 2009. The camera took a picture of an "E" pen tip, that is, a pen that has three tips at the end. That image was used as a base to compare subsequent images. In the base image, the coordinate system was set using the top corner of the end of the middle beam. The edge finding feature in the software also gave an angle. The same edge finding feature was used on subsequent images and the software calculated the difference in the position in the new coordinate system. The ball mount holder was taken out and put back into the fixture ten times.

4.2 Results

The fixture repeatability in X, Y, and z were calculated in the National Instruments Vision Builder image processing software. The camera took a picture of a NanoInk tip and the image processing software calculated the position of a tip relative to the center of the image. This image was used as the control and a coordinate system was set where the origin and the angle matched the position of the top left corner of the center beam. All subsequent images measured the position of the tip relative to this coordinate system.

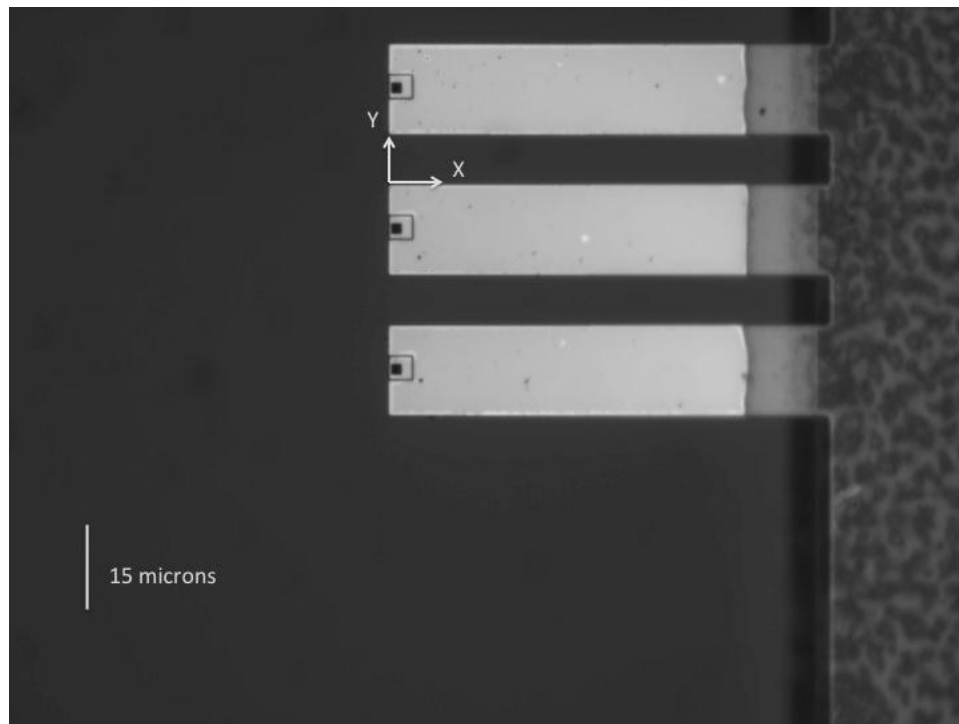


Figure 4.1: The Base Image of the “E” Pen Tip for Repeatability Testing.

The readings were normalized to the mean data values. The displacements from the average reading in X, Y, and z were plotted. The results of the repeatability testing are summarized in Figure 4.2 with error bars derived for a 95% confidence interval.

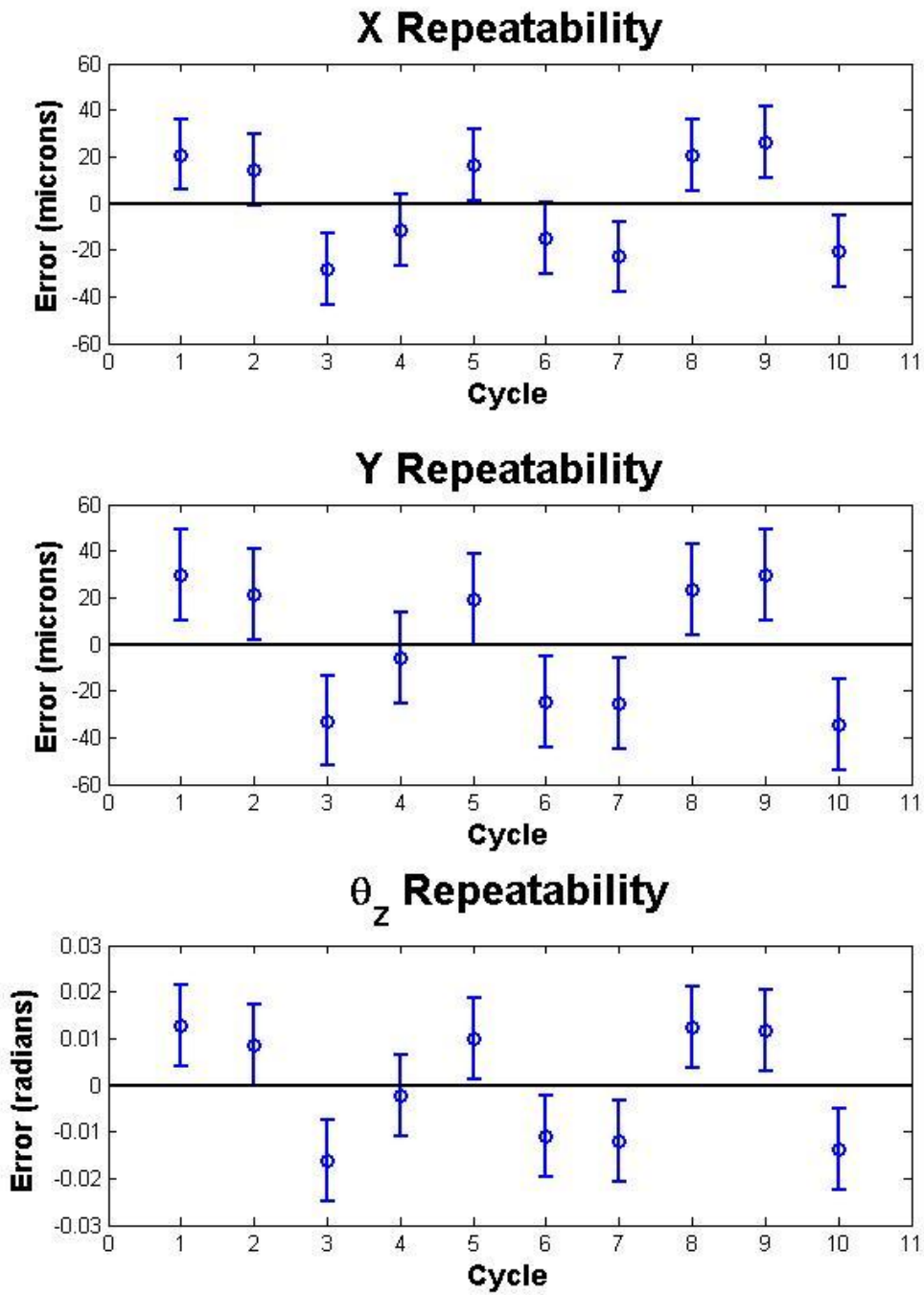


Figure 4.2: In-Plane Repeatability Results.

The two-dimensional translational repeatability in X and Y was calculated by taking the square root of the sum of the squared X and Y displacements. This translational repeatability was normalized to the mean and plotted in Figure 4.3.

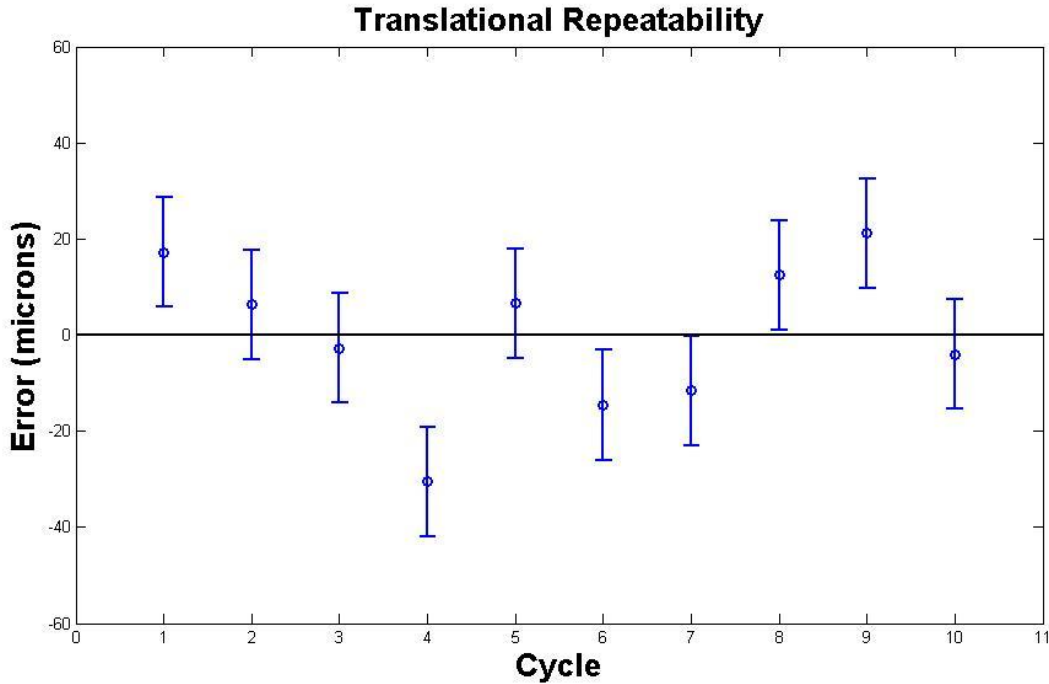


Figure 4.3: Translational Repeatability Results.

The repeatability was measured by one and three standard deviations from the mean. The 1 and 3 repeatability in the appropriate degrees of freedom are summarized in Table 4.1.

Table 4.1: 1 σ and 3 σ Repeatability Measurements.

	X (m)	Y (m)	z (rad)	2D (m)
1	21.3	27.3	0.0122	15.9
3	64.1	81.9	0.0367	47.8

4.3 Conclusion from Testing

The results show that the translational repeatability of the stage is within 60 microns and the angular repeatability is within 0.03 radians (approximately 2°). This is less than half of the original estimated requirements of 140 microns of translation and 0.1 radians of angularity for

the flexural stage. Thus, as long as the stage can travel twice the functional requirements, then the machine could align pen tips with accuracy and repeatability.

The repeatability error come mostly from two sources: the flexures on the in-plane holder are so stiff that Hertzian contact causes the ball mount itself to plastically deform, and the thin plate that the ball mount is pushed against on deforms like a trampoline, causing tip and tilt errors. This ball mount holder needs further optimization, but even this first iteration satisfies the functional requirements.

The outcome of this research included the design, fabrication and partial implementation of a machine that aligns a nanometer-sized pen tip with micron accuracy and repeatability. This can drastically improve the quality, rate, and flexibility while reducing the cost of dip pen nanolithography.

CONCLUSION

The purpose of this research was to develop a machine that makes miniature kinematic couplings for alignment for micro- and nanomanufacturing processes. The research covered here encompassed the modeling, optimization and fabrication of this machine. The import of this machine is that it allows for accurate, repeatable interchange of parts for various nanoscale instruments, such as Dip Pen Nanolithography (DPN) and Atomic Force Microscopy. This will improve the quality, rate, and flexibility of these instruments while decreasing the cost of alignment methods. This research was divided into two phases, design and implementation. The design, covered in chapter 2, contains the ideas and optimization of all of the parts that comprise the alignment machine. The implementation contains the fabrication, assembly, and testing of the parts of this machine.

5.1 Summary

This research was divided into two phases, design and implementation. The design, covered in chapter 2, contained the ideas and optimization of all of the parts that comprise the alignment machine. The implementation contained the fabrication, assembly, and testing parts of this machine. The design of this machine started as a fundamental idea to use a passive kinematic coupling for alignment for Dip Pen Nanolithography. Then the idea was further developed by holding the balls for the kinematic coupling half fixed, while moving the ball mount over it. Then the balls would be glued in place using UV-cured epoxy. From there, the idea evolved into parts that hold the ball mount and how that attached to a moving stage. The stage was given movement through the use of flexures. An appropriate topology was chosen through the use of FACT and the geometry was optimized through Finite Element Analysis. Voice coils actuated

the stage. The ball holder was developed and this also formed the ground of the machine. The ground was bolted to an optical table. The source of the ultraviolet light was UV flashlights and a mount was developed that held them in such a way that the light cones intersected on the main stage. Then the overhead camera was chosen and a mount was developed such that it allowed for fine adjustment for focusing. The camera was used to form a feedback loop for controlling the stage. The camera captured an image that was fed into image processing software that extracted the amount of travel needed for the stage. The amount of travel then turned into commands for a microcontroller to send to motor drivers, which moved the voice coils. All of these sub-assemblies were then stacked to form the full alignment machine.

With the design verified, the implementation followed. The machine was built using CNC machines including the Waterjet and the CNC Mill. After all of the parts were fabricated, they were assembled to form the mechanical part of the alignment machine. The camera was implemented, using screws to finely adjust the position of the camera for focusing. With the camera in focus, the basic mechanical apparatus could be tested. The camera was able to get a picture of the NanoInk DPN pen tips. The repeatability of the ball mount holder was tested and achieved a repeatability that was well within the functional requirements of the flexural stage. This is a promising result, however the rest of the apparatus remains to be tested.

5.2 Future Work

For future work, the electronics and the image processing software need to be integrated into the mechanical hardware. There are slight mechanical tweaks that need to be implemented, such as adding the tubes for maintaining the heights of the various components. They were not made because the CAD model only contains an estimate of these heights. The actual heights are obtained through testing. For example, the camera needs to be a certain height above the NanoInk tip that is to be found experimentally. The repeatability experiment could also be repeated to have more trials than ten to get more accurate results. The flexures in the in-plane ball mount holder need to be modified, as the flexures are too stiff. The flexures are pushing against the bumps so hard that Hertzian contact causes the ball mount to plastically deform. This plastic deformation ruins the repeatability of the ball mount holder. This geometric optimization of the flexures, as well as the minimization of Hertzian contact stresses can be done through the use of Finite Element Analysis.

Furthermore, the machine needs to be fully operational, that is, electronics and software need to be implemented. The electronic implementation includes testing and debugging the voice coil and motor drivers. The implementation for software includes finishing the LabView script that captures the necessary information for movement, and the Arduino software for turning these numbers into commands for the motor drivers. Then, the entire machine needs to be tested to ensure that it meets the functional requirements set by NanoInk.

REFERENCES

- [1] NanoInk, "What is Dip Pen Nanolithography (DPN)," accessed May 2012, <http://www.nanoink.net/technology.html>.
- [2] J. B. Hopkins, M. L. Culpepper, "Synthesis of precision serial flexure systems using freedom and constraint topologies (FACT)," *Precision Engineering*, vol. 35, pp. 638-649, 2011.
- [3] Tang, W.C., Nguyen, T., and Howe, R.T., 1989, "Laterally Driven Polysilicon Resonant Microstructures," *Sensors and Actuators A: Physical*, 20, pp. 256-32.
- [4] Grade, J.D., Jerman, H., and Kenny, T.W., 2003, "Design of Large Deflection Electrostatic Actuators," *J. of Microelectromechanical Systems*, 12(3), pp. 335-343.
- [5] F. Beyeler, S. Muntwyler, B. J. Nelson, "A Six-Axis MEMS Force-Torque Sensor With Micro-Newton and Nano-Newtonmeter Resolution," *Journal of Microelectromechanical Systems*, vol. 18, n. 2, pp. 433-441, 2009.
- [6] Luginbuhl, P., et al., 1996, "Piezoelectric Cantilever Beams Actuated by PZT Sol-gel Thin Film," *Sensors and Actuators A: Physical*, 54, pp. 530-535.
- [7] Chen, S.C. and Culpepper, M. L., 2006, "Design of a Six-axis Microscale Nano-positioner - Hexflex," *J. of Precision Eng.* 30(3), pp. 315-24.
- [8] Miyajima, H., et al., 2003, "A MEMS Electromagnetic Optical Scanner for a Commercial Confocal Laser Scanning Microscope," *J. of Microelectromechanical Systems*, 12(3), pp. 243-251.
- [9] Bell, D.J., et al., 2005, "MEMS Actuators and Sensors: Observations on Their Performance and Selection for Purpose," *J. Micromech. Microeng.*, 15, pp. 153-164.
- [10] PixeLINK, "PL-B777 Machine Vision Camera, Microscope Camera from PixeLINK," accessed May 2012, <http://www.pixelink.com/products/PL-B777-details.aspx>.